Dept. of Mech. Eng.
CUET

Published Online April 2017 (http://www.cuet.ac.bd/merj/index.html)

Mechanical Engineering Research Journal

Vol. 10, pp. 47-50, 2016

ISSN: 1990-5491

FLUID FLOW ANALYSIS IN ELECTROSTATIC PRECIPITATOR OF A COAL FIRED POWER PLANT CONSIDERING ELECTRODE WITH TWO DIFFERENT SHAPE OF BAFLLES

A. S. M. Sayem*, M. M. K. Khan, M. G. Rasul and N. M. S. Hasan

School of Engineering and Technology, Central Queensland University, QLD 4702, Australia

Abstract: Sustainable clean energy production is one of the important challenges in the modern world, especially in case of coal based power generation it is more applicable as it involves a huge amount of emission including hazardous particulate matters. Coal fired power plant is one of the main sources of electrical energy due to the low cost of coal compared to other fossil fuels and proven reserves in Australia and in many countries of the world. However, a major problem of the coal fired power plant is the exhaust emission of fine particulate matter. Among available technologies, 'Electrostatic Precipitators (ESP)' are the most reliable control devices to capture the fine particles and its efficiency is almost 99% or above. Most of the coal power plants and other process industries generally use ESP because of their effectiveness and reliability in controlling particulate matters. To capture the particulate matter through ESP, the electrode diameter and shapes of baffles is very important. In this study, two different shapes of baffles inside the ESP including electrode have been considered to assess their influence on the flow pattern using computational fluid dynamics (CFD) code 'ANSYS FLUENT'. Due to different shapes of baffles and electrodes, the flow distribution was changed inside the ESP which increases the residence time of flue gases. The results indicate that the proposed shapes can influence to collect more fine particles. The influence of the presence of the electrodes and back pressure on the flow phenomena is discussed.

Keywords: *Electrode diameter, Back pressure, Residence Time, Baffles.*

1. INTRODUCTION

Most of the coal power plants and other process industries generally use Electrostatic Precipitators (ESP) because of their effectiveness and reliability in controlling emission of particulate matter [1]. Fig. 1 shows a typical arrangement of an ESP in the power plant. Before going into the environment, flue gas flows through the ESP where particles are collected. The ESP can be used as a cleaning device. For separating the dust particles from the flue gas, an electrical field is created and used by the ESP. A rectangular collection chamber consists of an inlet and outlet convergent duct. The inlet and outlet convergent duct are known as the inlet and outlet evase which are the key components of an ESP. For flow distribution, perforated plates are placed inside the inlet and outlet evase. A number of discharge electrodes (DE) and collection electrodes (CE) are positioned inside the collection chamber. Fig. 2 presents a small section of a typical wire-plate ESP channel where a set of discharge electrodes is suspended vertically and gas flow through an ESP.

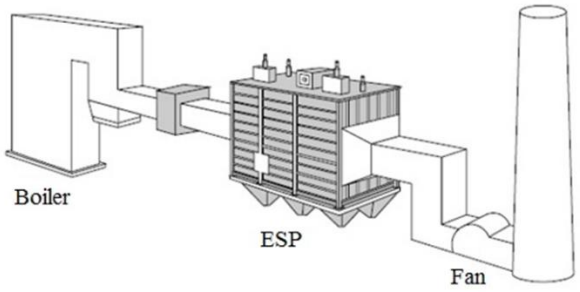

Fig. 1 A typical arrangement of an ESP in the power plant [1].

* **Corresponding author:** Email: a.sayem@cqu.edu.au; Tel: +61 7 49232123 | X 52123

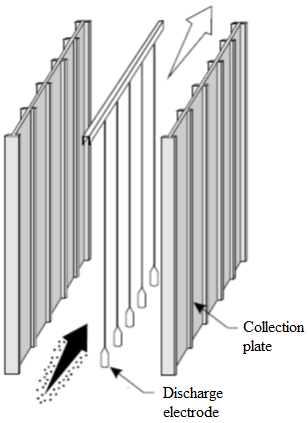

Fig. 2 A typical wire-plate ESP channel where a set of discharge electrodes is suspended vertically and gas flow through an ESP [1].

2. GEOMETRY

A laboratory scale ESP model, geometrically similar to an industrial ESP, was designed and fabricated by Shah *et al.* [5, 6] at the Thermodynamics Laboratory of Central Queensland University, Australia to examine the flow behaviour inside the ESP. This laboratory scale ESP consisted of a rectangular collection chamber and an inlet evase and an outlet evase. The current study focuses on further improvement of the flow behaviour inside the ESP and has taken into account the rectangular collection chamber as a rectangular duct for simplicity of the model geometry. This is because the dust particle separation from the flue gas and the collection of dust particles usually occur inside the rectangular duct. The Geometry is created in Design Modeller of ANSYS Fluent and further processing is done for meshing and refinement The geometry is shown in Fig. 3(a) and Fig. 3(b). ANSYS code 'FLUENT' is used for numerical simulation of fluid flow behavior

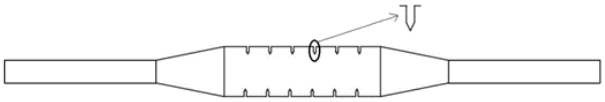

Fig. 3(a) ESP containing arrow shape baffles.

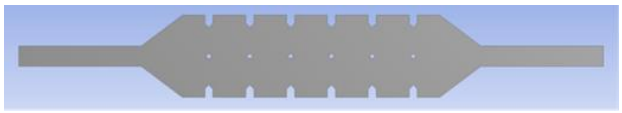

Fig. 3(b) ESP containing arrow shape baffles with electrode.

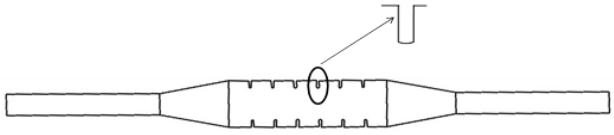

Fig. 3(c) ESP containing circular shape baffles with electrode.

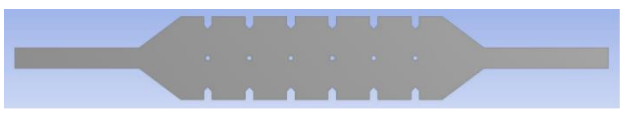

Fig. 3(d) ESP containing circular shape baffles with electrode.

The ESP considered in this paper has a single chamber. As seen from Fig. 3(a), six arrow shape baffles were inserted in two opposite sidewalls. The arrow shape baffles with electrode are shown in Fig. 3(b). The circular shape baffles and with electrode are shown in Fig. 3(c) and Fig. 3(d) respectively. The length, width and height of the duct are: 157.5 cm, 60 cm and 50 cm respectively. The baffles are equally spaced and the distance between two baffles is 20 cm. Each baffle has a height of 50 cm, width of 5 cm and length of 2.5 cm. The diameter of electrodes are 2.79 cm respectively.

It is noted that the results of the impact of the baffles on the flow are discussed on a qualitative basis since more results are required for a quantitative analysis.

3. NUMERICAL APPROACH AND SIMULATION PROCEDURE

As mentioned earlier, the mesh created by Design Modeller is exported to ANSYS to discretize the fluid domain into small cells to form a volume mesh or grid and set up appropriate boundary conditions. Numerical computation of fluid transport includes continuity, momentum and turbulence model equations. The flow properties and equations are solved and analyzed by CFD code "FLUENT" [7].

Continuity equation:

$$\frac{\partial \bar{u}}{\partial x}+\frac{\partial \bar{v}}{\partial y}+\frac{\partial \bar{w}}{\partial z}=\frac{\partial(u_i)}{\partial x_i}=0 \quad (1)$$

Momentum Equation:

$$\frac{\partial}{\partial t}(\rho u_i)+\frac{\partial}{\partial x_j}(\rho u_i u_j)=-\frac{\partial p}{\partial x_j}+\frac{\partial \tau_{ij}}{\partial x_j}+\rho g_i+F_i \quad (2)$$

In this equation, p is static pressure and self-defined source term are contained in *Fi*, Stress tensor is determined by the following equation:

$$\tau_{ij}=\left[\mu\left(\frac{\partial u_i}{\partial x_j}+\frac{\partial v_j}{\partial x_i}\right)\right]-\frac{2}{3}\mu\frac{\partial u_i}{\partial x_i}\delta_{ij} \quad (3)$$

$$\frac{\partial}{\partial t}(\rho k)+\frac{\partial}{\partial x_j}(\rho k u_j)=\frac{\partial}{\partial x_j}\left[\left(\mu+\frac{\mu t}{\sigma k}\right)\frac{\partial k}{\partial x_j}\right]+(G_k+G_B-Y_M)-\rho\epsilon+S_k \quad (4)$$

$$\frac{\partial}{\partial t}(\rho \epsilon)+\frac{\partial}{\partial x_j}(\rho \epsilon u_i)=\frac{\partial}{\partial x_j}\left[\left(\mu+\frac{u_t}{\sigma \epsilon}\right)\frac{\partial \epsilon}{\partial x_j}\right]+C_{1\epsilon}\frac{\epsilon}{k}(G_k+C_{3\epsilon}G_b)-C_{2\epsilon}\rho\frac{\epsilon^2}{k}+S_\epsilon \quad (5)$$

where u, v, w is each component of gas velocity, (m/s) and μ, μ_t are molecular viscosity and kinetic viscosity (Pa.s) respectively; ρ (kg/m^3) is fluid density, G_k represents turbulent energy generated by mean velocity gradient; G_B is turbulent energy generated by buoyancy; Y_M represents pulsation expansion in turbulent model of compressible flow; $C_{1\epsilon}$, $C_{2\epsilon}$ and $C_{3\epsilon}$ are empirical constant; σk and $\sigma \epsilon$ are corresponding turbulent Prandtl number in k-equation and ε-equation; $S_k$and S_ε are self-defining source term; $C_{1\epsilon}$ = 1.44, $C_{2\epsilon}$ = 1.92, $C_{3\epsilon}$ = 0.09, σk =1.0, $\sigma \epsilon$ = 1.3 [8]

Realizable k-ϵ model was selected in this study, as it differs from the others k-ϵ model in two important ways. Firstly, the realizable k - ϵ model contains a new formulation for the turbulent viscosity. Secondly, a new transport equation for the

dissipation rate, ε (dissipation rate of turbulent kinetic energy, m^2/s^3), has been derived from an exact equation for the transport of the mean-square velocity fluctuation [7]. The turbulent kinetic energy k (turbulent kinetic energy, m^2/s^2) and its dissipation rate ϵ for Realizable $k-\epsilon$ model are obtained from the transport equation (4) and equation (5) respectively [7, 8].

4. MESH GENERATION AND BOUNDARY CONDITION

Three dimensional simplified model of ESP was employed in this study to investigate the flow phenomena. ANSYS 15.0 was used to establish models for calculating regions where unstructured grids were generated and finally, after resizing and refinement, structured grid was obtained. The number of nodes and cells obtained were 54265 and 96336 for arrow shape baffles and 54136, 96534 for circular shape baffles. Air was used as a fluid and its acquiescent properties were maintained with constant velocity. The boundary conditions were applied as follows: inlet velocity was considered as constant velocity which was 10 m/s, the outlet boundary condition was pressure outlet and "No slip" (velocity at the wall to be zero) boundary condition was imposed on the side walls of the ESP including baffles and electrodes.

The finite volume method was used to discretise the partial differential equations of the model. The Semi-Implicit Method for Pressure-Linked Equations (SIMPLE) scheme was used for pressure–velocity coupling and the second order upwind scheme was used because of its combination of accuracy and stability and as this scheme interpolates the variables on the surface of the control volume. Turbulent kinetic energy k and turbulent dissipation rate ε were considered as a second order upwind for better simulation accuracy.

In order to compute the results, all simulations were carried out on an Intel Core i5 processor computer that has 2.80 GHz processor and 8.00 GB of RAM, 64-bit operating system.

5. RESULTS AND ANALYSIS

The assembled graphs below show the simulation results of velocity and pressure distribution for circular and arrow shape respectively. Six baffles were inserted into each wall in air flow distribution plates. In the following Fig.s, the influence of baffle and electrode on forming skewed air flow pattern is considered only.

The Figs. 5(a) and 5(b) show the contour of the velocity distribution for circular shape baffles with and without electrode. Fig. 5(c) is the pressure distribution of circular shape baffles in ESP respectively. Fig. 5(d), Fig. 5(e) and Fig. 5(f) are the velocity distribution and the pressure distribution for arrow shape baffles respectively.

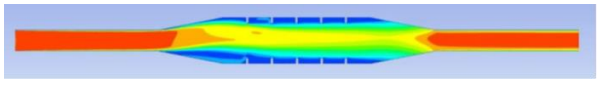

Fig. 5(a) Velocity distributions for circular shape baffles.

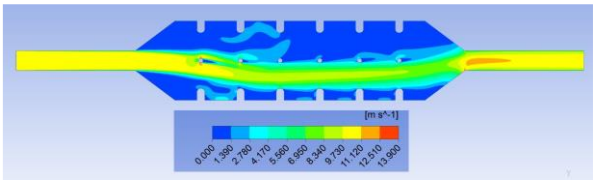

Fig. 5(b) Velocity distributions for circular shape baffles with electrode.

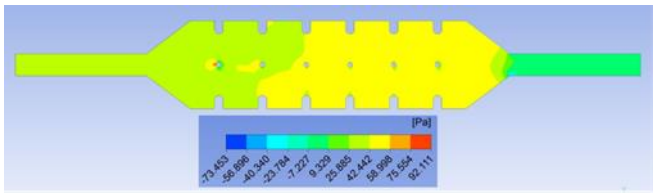

Fig. 5(c) Pressure distribution for arrow shape baffles with electrode.

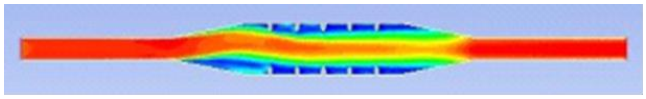

Fig. 5(d) Velocity distributions for arrow shape baffles.

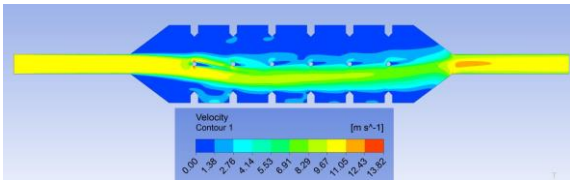

Fig. 5(e) Velocity distributions for arrow shape baffles with electrode.

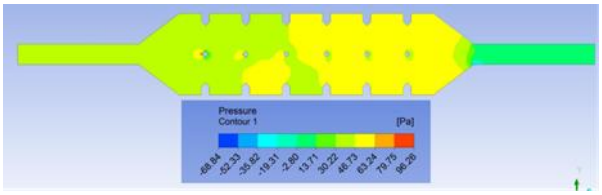

Fig. 5(f) Pressure distributions for arrow shape baffles with electrode.

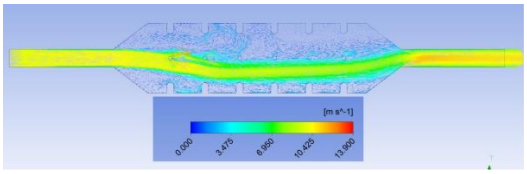

Fig. 5(g) Velocity vector for arrow shape baffles with electrode.

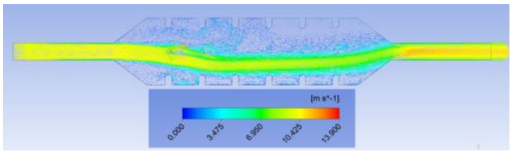

Fig. 5(h) Velocity vector for circular shape baffles with electrode.

It is seen from these Figures that the velocity distribution pattern is quite different because of the changing shapes of baffles and the effect of electrode. In case of circular shape baffles, the velocity stream line is changed more frequently in comparison with the velocity distribution of arrow shape baffles even though the velocity distribution of arrow shape baffles maintains a smooth stream line. Observing the velocity patterns, circular shape baffles have greater potential to capture

particulate matter since the velocity changes more frequently causing pressure fluctuation and hence falling particles from the flow. It is observed from Fig. 5(a) that the area near the baffles has almost zero velocity, which enables to collect finer particles due to an increase in residence time. Fig. 5(b) and Fig. 5(e) indicate that there is a possibility to create vacuum on the right side of electrode which will impact on uniform ionization. But it could be more accurately discussed with the adding of electrostatic field model that has not yet been studied. However, it increases drag force for upcoming flue gases. The velocity pattern of arrow shape baffles keeps a smooth centerline velocity stream which reduces drag force for upcoming flue gases and also decreases residence time due to the smooth velocity flow which is shown in Fig. 5(b). Fig. 5(c) and Fig. 5(f) show the pressure distribution for circular shape and arrow shape baffles respectively. In case of circular shape, pressure increases gradually and reaches a maximum level at the middle of ESP, on the other hand, a mixed pressure distribution is obtained in arrow shape baffles. From these Figures it is also observed that near the back face of the baffles, the velocity is small or near zero. This indicates that more dust is likely to be settled and accumulated in this zone. Fig. 5(g) and Fig. 5(h) show the velocity vector of arrow shape and circular shape baffles with electrode respectively.

6. CONCLUSION AND RECOMMENDATION

The CFD analysis of two different shapes baffles ESP shows some encouraging and favorable result. The summery that can be drawn is as below:

- Qualitative analysis of two different flow pattern shows that the installed baffles form skewed gas flow. This formation is influenced by baffles shape, interval between two baffles and electrode size as well as electrode position. Skewed gas flow also increases the residence time of the flue gas inside the duct leading to more dust collection. Further study will be conducted on the gap between two opposite baffles and position of electrode placement.
- Velocity distribution indicates that smooth velocity pattern is obtained in case of arrow shape baffles whereas circular shape baffles offer comparatively lower velocity adjacent to the baffles, which is more suitable for dust collection. Further study is needed to examine the residence time and drag force for these baffles by varying electrode position.
- The dynamics of formation of the skewed flow is complicated and is not quantitatively analyzed. However, qualitatively, it shows the creation of vortex flow near the baffles and existence of a near zero velocity close to the wall of the baffles, which suggests an improvement of the dust collection efficiency.
- Further investigation is required to determine the strength of vortex flow which is also influence by application of electrostatic field around electrode.

ACKNOWLEDGEMENTS

This research was financially supported by Central Queensland University through the Strategic Research Scholarship Scheme.

REFERENCES

[1] APTI, Air Pollution Training Institute (APTI) Course SI: 412B, in, U.S Environmental Protection Agency, 1998.

[2] M. Hu, X. Sun, C. Ma, Y. Liu and L.-q. Wang, "Numerical Simulation of Influence of Baffler in Electric Field Entrance to Form Skewed Gas Flow".

[3] L. Morawska, V. Agranovski, Z. Ristovski and M. Jamriska, "Effect of face velocity and the nature of aerosol on the collection of submicrometer particles by electrostatic precipitator", Indoor air, Vol. 12, pp. 129-137, .2002.

[4] A. Jaworek, A. Krupa and T. Czech, "Modern electrostatic devices and methods for exhaust gas cleaning: A brief review", Journal of Electrostatics, Vol. 65, pp. 133-155, 2007.

[5] S. M. E. Haque, M. G. Rasul, A. V. Deev, M. M. K. Khan and N. Subaschandar, "Flow simulation in an electrostatic precipitator of a thermal power plant", Applied Thermal Engineering, Vol. 29, pp. 2037-2042, 2009.

[6] S. M. Haque, M. Rasul, M. M. K. Khan, A. Deev and N. Subaschandar, "Influence of the inlet velocity profiles on the prediction of velocity distribution inside an electrostatic precipitator", Experimental Thermal and Fluid Science, Vol. 33, pp. 322-328, 2009.

[7] ANSYS FLUENT 12.0 Theory Guide.

[8] F. Dubois and W. Huamo, "New advances in computational fluid dynamics—theory, methods and applications [M]", in Beijing: Higher Education Press, 2001.

[9] J. Podlinski, A. Niewulis, J. Mizeraczyk and P. Atten, "ESP performance for various dust densities", Journal of Electrostatics, 66, pp. 246-253, 2008.

[10] C. Ruttanachot, Y. Tirawanichakul and P. Tekasakul, "Application of electrostatic precipitator in collection of smoke aerosol particles from wood combustion", Aerosol and Air Quality Resarch, Vol. 11, pp. 90-98, 2011.

[11] B. Y. Guo, Q. F. Hou, A. B. Yu, L. F. Li and J. Guo, "Numerical modelling of the gas flow through perforated plates", Chemical Engineering Research and Design, Vol. 91, pp. 403-408, 2013.

[12] Z. Al-Hamouz, "Numerical and experimental evaluation of fly ash collection efficiency in electrostatic precipitators", Energy Conversion and Management, Vol. 79, pp. 487-497, 2014.

[13] A. S. M. Sayem, M. M. K. Khan, M. G. Rasul, M. T.O. Amanullah and N. M. S. Hassan, "Effects of baffles on flow distribution in an electrostatic precipitator (ESP) of a coal based power plant", in: 6th BSME International Conference on Thermal Engineering (ICTE 2014), Procedia Engineering, pp. 8, Dhaka, Bangladesh, 2015.